Available online at www.sciencedirect.com
ScienceDirect
Polymer 48 (2007) 2910–2918
polymer
www.elsevier.com/locate/polymer

Surface immobilization of polymer brushes onto porous poly(vinylidene fluoride) membrane by electron beam to improve the hydrophilicity and fouling resistance

Fu Liu, Chun-Hui Du*, Bao-Ku Zhu, You-Yi Xu

Institute of Polymer Science, Zhejiang University, Yuquan, Hangzhou 310027, People's Republic of China

Received 21 January 2007; received in revised form 3 March 2007; accepted 12 March 2007
Available online 15 March 2007

Abstract

Poly(vinylidene fluoride) (PVDF) membrane was pre-irradiated by electron beam, and then poly(ethylene glycol) methyl ether methacrylate (PEGMA) was grafted onto the membrane surface in the aqueous solution. The degree of grafting was significantly influenced by the pH value of the reaction solution. The surface chemical changes were characterized by the Fourier transform infrared attenuated total reflection spectroscopy (FTIR-ATR) and X-ray photoelectron spectroscopy (XPS). Combining with the analysis of the nuclear magnetic resonance proton and carbon spectra (^{1}H NMR and ^{13}C NMR), PEGMA was mainly grafted onto the membrane surface. Morphological changes were characterized by scanning electron microscopy (SEM) and atomic force microscopy (AFM). The porosity and bulk mean pore size changes were determined by a mercury porosimeter. The surface and bulk hydrophilicity were evaluated on the basis of static water contact angle, dynamic water contact angle and the dynamic adsorption process. Furthermore, relative high permeation fluxes of pure water and protein solution were obtained. All these results demonstrate that both hydrophilicity and fouling resistance of the PVDF membrane can be improved by the immobilization of hydrophilic comb-like polymer brushes on the membrane surface.

Keywords: PVDF membrane; Electron beam; Hydrophilicity

1. Introduction

PVDF is one of the remarkable polymer materials for separation membranes. It has excellent chemical stability, thermal stability, low dielectric constants and low surface energy [1]. PVDF has been extensively applied in many membrane areas such as membrane distillation [2–5], membrane absorption [6,7], fuel cell [8–10], gas separation [11–13], pervaporation [14–16]. However, PVDF has some limitations in waste water treatment due to its hydrophobicity. Firstly, the hydrophobic membrane has the lower surface energy and the higher water contact angle, so the water flux is very low. Secondly, the hydrophobic membrane is susceptible to the proteins or oils fouling during the microfiltration or ultrafiltration process. The membrane fouling mechanisms are an important research field [17–19]. In most fouling cases, both internal fouling and external fouling occur during the microfiltration and ultrafiltration processes. Protein adsorption, aggregation and denaturation play an important role with the consequence of the reduction of membrane performance [20–22]. So the membrane permeation flux and selectivity will be dramatically reduced due to either the built-up of an additional barrier layer or the failure of the barrier.

Mathias Ulbricht has provided a comprehensive overview on the development of polymeric membranes having advanced or novel function in the various membrane separation processes. Fouling-resistant surface functional membrane could be obtained by various methods to improve the membrane hydrophilicity [23]. Physical blending is a fairly easy method. The addition of poly(methyl methacrylate) (PMMA) [24–26], polyacrylonitrile (PAN) [27], Al_2O_3 [28] can improve the

* Corresponding author. Tel./fax: +86 571 87953011.
E-mail address: duchunhui@zju.edu.cn (C.-H. Du).

0032-3861/$ - see front matter © 2007 Elsevier Ltd. All rights reserved.
doi:10.1016/j.polymer.2007.03.033

hydrophilicity and the antifouling property. However, only few additives are compatible with PVDF membrane to some extent. Therefore, there has been much attention in synthesizing PVDF amphiphilic graft copolymers by living/controlled free-radical polymerization in recent years [29,30]. These amphiphilic copolymers with good compatibility with matrix PVDF were blended with PVDF to provide functional membranes. The surface segregation of the hydrophilic side chains delivered the desired protein fouling resistance of the membrane. However, the catalysts or ligands that are required in living free-radical polymerization cannot be completely removed from copolymers. In addition, the living polymerization efficiency needs to be further improved. Compared to physical blending, surface grafting is a versatile means to modify PVDF membrane, which will not only preserve the bulk structure of the membrane but also achieve the novel functionality of the grafted chains. Since various hydrophilic monomers are covalently bonded with the membrane, the improved properties through surface grafting method could remain stable for long. As the carbon–fluorine bond energy (530.5 kJ/mol) is the strongest one between carbon and other elements [31], and the larger size fluorine atoms can also protect the carbon backbone of PVDF from harsh chemical attack. Some common techniques including chemical treatment, UV, plasma have some limitations to activate the PVDF membranes due to their lower energy. *G* value (the number of species formed on the deposition of 100 eV of energy) of PVDF under vacuum at room temperature is 3.3, so the high energy electron beam is efficient and practical to modify either the surface or bulk properties of PVDF membrane [32]. Moreover, the high energy electron beam radiation technique has higher dose rate and the irradiation process can be controlled easily. The radiation technique is clean because, unlike other polymerization methods, radiation grafting reaction does not require any additives or catalysts. Since the monomers are not directly exposed to radiation, the pre-irradiation method produces less homopolymers than the simultaneous or peroxy/hydroperoxy irradiation method does.

The reactivity nature of the monomer to be grafted has a very important effect on the efficiency and the uniformity of the grafted chains. A very large variety of functional monomers have been grafted on PVDF to obtain desired properties, such as acrylic acid/sodium 4-styrenesulfonate [33,34], *N*-isopropylacrylamide [35], styrene [36], etc. Most of the grafted chains from above monomers are linear. A potential disadvantage is that the grafted chains may grow long when high degree of grafting is needed, and consequently, the long polymer straight chains may minimize or even plug the pores of the porous membrane. So it is significant to study special grafted polymer architectures on the membrane surface or in the pores of the porous membrane. The special grafted polymer chains include a controlled degree of grafting, a narrow chain length distribution and branched and/or cross-linked polymer architecture. The branching topology may vary from the relatively simple cases of comb-like, star-like, and H-like polymers, to the more complex cases of hyperbranched polymers and dendrimers. Especially for the comb-like grafted polymers, we can obtain the desirable hydrophilicity of the membrane even at the low degree of grafting, because with the right chain length the hydrophilic grafted side chains can spread out on the membrane surface.

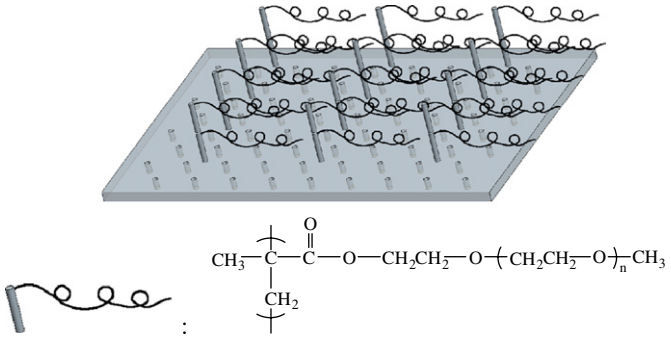

Fig. 1. Schematic diagram showing the grafting of PEGMA on the PVDF membrane.

In the present study, we aim to prepare poly(ethylene glycol) methyl ether methacrylate grafted PVDF porous membrane by the pre-irradiation method with the high energy electron beam. The PVDF porous membrane is pre-irradiated with the high energy electron beam, and then the activated membrane reacts with the hydrophilic monomer of poly(ethylene glycol) methyl ether methacrylate in aqueous solution. So we can obtain the modified PVDF membrane with the immobilization of hydrophilic comb-like polymer brushes on the membrane surface. Fig. 1 is a schematic diagram for the modified PVDF membrane. The chemical structure changes of the grafted membrane were investigated by FTIR-ATR, XPS and NMR. The surface morphologies were studied by SEM and AFM. The hydrophilicity was evaluated by the measurements of both static contact angles and dynamic contact angles. The water flux and filtration experiments were also performed.

2. Experimental section

2.1. Materials and reagents

PVDF (FR-904, $M_n = 380{,}000$) was purchased from Shang-Hai New Materials Co. *N*,*N*-Dimethylacetamide (DMAc) was purchased from ShangHai 3S Co. Polyethylene glycol (PEG-600) was obtained from ShangHai Chemical Co. Poly(ethylene glycol) methyl ether methacrylate (PEGMA, $M_n = 475$ and 1100) was purchased from Sigma–Aldrich. Albumin, bovine serum (BSA, $M_w = 67$ kDa) was purchased from Sino-American Biotechnology Co. Phosphate buffered saline (PBS, 0.01 M) was prepared by dissolving pre-weighed quantities of potassium dihydrogen phosphate (KH_2PO_4) and disodium hydrogen phosphate ($Na_2HPO_4 \cdot 12H_2O$) in deionized water.

2.2. Preparation and irradiation of PVDF membrane

PVDF porous membrane was prepared by the phase inversion method from the casting solution (PVDF/PEG-600/DMAc = 14/5/81). The typical PVDF membrane irradiation process was as follows: membranes were cut (9.5×12.5 cm^2)

and weighted, and then they were placed in thin polyethylene plastic bags, which were flushed with N_2 for 30 min and then thermally sealed. PVDF membranes within the bags were exposed vertically to high energy electron beam direction at 25 °C. The irradiation dose was 100 kGy and the beam current was 0.2 mA. The irradiated PVDF membranes were stored at −20 °C before grafting.

2.3. Grafting copolymerization of PVDF membrane

The irradiated PVDF membrane was quickly immersed into the grafting aqueous solution containing PEGMA (0.2 M). The solution was deaerated by bubbling nitrogen for 15 min in a glass reaction tube. The tube was sealed and put into a water bath at 70 °C for desirable time. The pH value of reaction solution was adjusted by adding HCl. After completion of the grafting reaction, the membrane was washed in ultrasonic water bath at 60 °C for 24 h to ensure no homopolymers were left in the membrane. The grafted membrane was dried at 50 °C in vacuum to constant weight. The degree of grafting was determined as the weight increase of the membrane according to the following equation:

$$\text{degree of grafting } (G\%) = \frac{W_g - W_o}{W_o} \times 100$$

where W_g is the weight of the grafted membrane and W_o is the weight of the original membrane.

2.4. Chemical composition characterizations

To study the surface chemical composition changes of PVDF membrane, FTIR-ATR spectroscopy was carried out on a Bruker Vector 22 FT-IR spectrophotometer. The spectra were measured in the wave number range of 4000–500 cm^{-1}. The spectra were collected by cumulating 32 scans at a resolution of 2 cm^{-1}.

The X-ray photoelectron spectroscopy (XPS, Perkin–Elmer Instruments, USA) was used to further study the PVDF membrane surface chemical composition change. It was equipped with Al Kα at 1486.6 eV and 300 W power at the anode. The energy scale of the spectrometer was calibrated using the lowest bonding energy component present in the superficial layer. A survey scan spectrum was taken and the surface elemental composition was calculated from the peak area with a correction for atomic sensitivity. The error in all the binding energy (BE) values reported is ±0.1 eV.

Nuclear magnetic resonance (NMR) spectra were performed on a Varian-300 instrument (300 and 75 MHz for ^1H and ^{13}C, respectively) with deuterated DMSO as the solvent. The grafted PVDF membrane was dissolved in the DMSO in the NMR tube. The operation was run at room temperature. The PEGMA content of the grafted membrane was determined by ^1H NMR.

2.5. Membrane morphology and structure characterization

The surface and cross-section morphologies of the membranes were examined by scanning electron microscopy (SEM, Sirion-100 FEI). The cross section was fractured in liquid nitrogen. A thin layer of gold was sputtered on the membrane surface and cross section before measurement.

An atomic force microscopy (AFM, Seiko instrumental SPA 400, Japan) was also used to further study the surface topography change of the membrane. AFM images were acquired in the tapping mode with silicone tip cantilevers having a force constant of 20 mN/cm.

The mean pore size and bulk porosity were measured with a mercury porosimeter (AutoPore IV9500, Micromeritics).

Thermal behavior of PVDF and PVDF-*g*-PEGMA membrane was investigated by a differential scanning calorimetry (DSC-7, Perkin–Elmer Cetus Instruments, Norwalk, CT). For DSC measurements, the temperature was raised from 50 to 200 °C at a heating rate of 10 °C/min under nitrogen atmosphere. The melting temperature (T_m) and the heat of fusion (ΔH_f) were determined from the obtained melting endotherms. The weight percent PVDF crystallinity in PVDF-*g*-PEGMA membrane was calculated from the ratio of the heat melting from the DSC thermograms and the reported heat of fusion of PVDF (101.5 J/g) [37], normalized by the weight fraction of PVDF in PVDF-*g*-PEGMA membrane determined from NMR.

2.6. Hydrophilicity and filtration performance characterization

The apparent static contact angle, dynamic contact angle and water drop adsorption on the membrane were measured at 25 °C using a sessile-drop technique with a video-based high speed contact angle measuring device (OCA20, Germany Dataphysics). One microliter of deionized water was dropped onto the membrane upper surface, which has the smaller pore size and determines the separation performance. For dynamic contact angles, the advancing, the receding and the hysteresis contact angles were measured. For the water drop adsorption process, the change of the contact angles was recorded as a function of the drop age on the surface to determine the time required for the adsorption of the drop.

Water flux experiments were performed in a homemade dead-end filtration apparatus similar to the one described previously [38]. All filtration experiments were carried out at 25 °C. The experimental protocol was as follows: in the first 30 min, the membrane was pre-compacted at 0.15 MPa pressure of transmembrane. Then the pure water flux was recorded at 0.1 MPa for every 5 min. After the pure water flux measurements, the deionized water was exchanged with 1.0 g/L BSA solution in PBS for the fouling-resistance test.

3. Results and discussion

3.1. Dependence of the degree of grafting on reaction conditions

Fig. 2 shows that the pH value of the solution influences the grafting reaction significantly. The degree of grafting decreases with increasing pH of the reaction solution. The degree of grafting varies from 21.0 at pH 1.0 to 1.1 at pH 10.3. In the

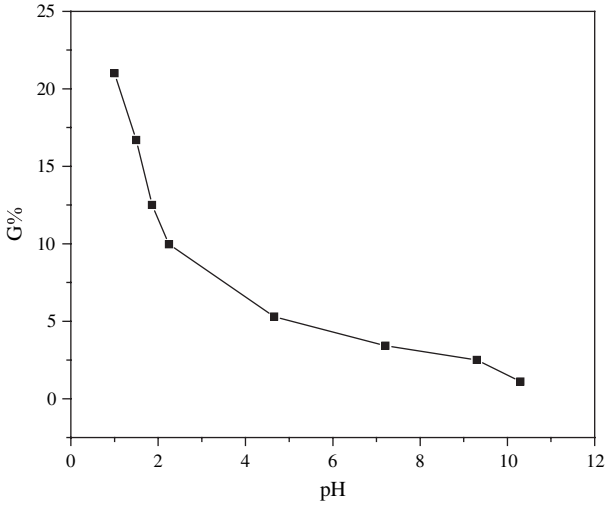

Fig. 2. Effect of pH value of the reaction solution on the degree of grafting.

reaction solution, the hydrophobic PVDF surface is usually incompatible with the hydrophilic monomer PEGMA. At lower pH values, the molecular chains of PEGMA monomers show the hydrophobic structure and have a better compatibility with the hydrophobic PVDF membrane with the free radicals. So the monomers easily diffuse onto the membrane surface. Since the surface grafting is a monomer diffusion-controlled reaction, the degree of grafting is higher at lower pH values [39]. At higher pH values, the $-CH_2CH_2O-$ side chains of the monomer change into stretching state and show the hydrophilicity, increasing the viscosity of the reaction solution and then depressing monomer diffusion [40]. So the degree of grafting is lower.

The dependence of the degree of grafting on the monomer concentration is shown in Fig. 3. It is obvious that the DOG increases rapidly with increasing the concentration of PEGMA monomer and then level off and reaches a saturation state. At 0.2 M, the gel effect which is the result of a sudden self-acceleration of polymerization reaction enhanced by the decrease of the termination rate due to an increased reaction solution viscosity will be considered. When the monomer concentration is above 0.2 M, monomer homopolymerization will increase the viscosity of the reaction solution and limit monomer's diffusion rate onto the living sites of the PVDF membrane, thus it retards the degree of grafting. Therefore, graft copolymerization in this system strongly depends on the availability of the monomer in the grafting sites, which is known as the monomer diffusion-controlled mechanism [39].

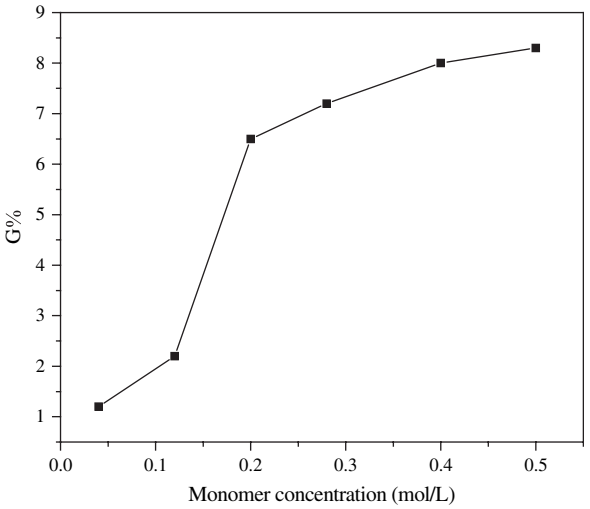

Fig. 3. Effect of monomer concentration on the degree of grafting.

3.2. Structure characterization of the membranes

Fig. 4 shows the respective FTIR-ATR spectra of (a) original membrane and (b) 6.63 wt% PEGMA grafted PVDF membrane. The appearance of the typical bands at 1727 and 1106 cm^{-1} is assigned to the C═O and C−O−C functional groups. The lacking of the carbon−carbon double bond (C═C) at 1641 cm^{-1} indicates that PEGMA has been grafted onto PVDF membrane surface through carbon−carbon double bond polymerization and no more unreacted monomers were left on membrane surface.

Fig. 5 shows the typical XPS spectra of (a) original membrane and (b) 6.63 wt% PEGMA grafted PVDF membrane. Both membranes show the peaks corresponding to C1s (binding energy, 290.7 eV) and F1s (binding energy, 694.5 eV) typically for PVDF. Comparing with the original membrane, the grafted one shows an extra peak corresponding to O1s (binding energy, 535.0 eV). Especially the surface oxygen content (13.98 mol%) increases significantly due to the grafting of the PEGMA on the membrane surface. Fig. 6 shows (a) the C1s core level scan spectra and (b) the O1s core level scan spectra of the PVDF-*g*-PEGMA membrane. C1s could be resolved into five peaks corresponding to CH, C−COO, CH_2, C−O, COO and CF_2 with binding energy at 288.5, 289.2, 290.0, 290.0, 292.5 and 294.5 eV, respectively. The emergences of C−COO, C−O and COO peaks in C1s core level scan spectra indicate that PEGMA chains have been grafted

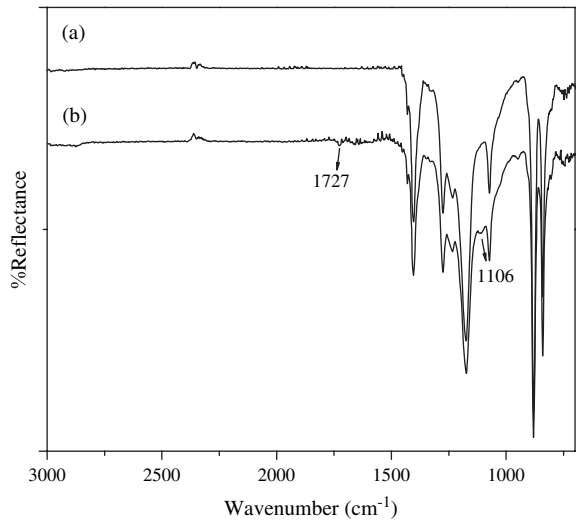

Fig. 4. FTIR-ATR spectrum of (a) original membrane and (b) 6.63 wt% PEGMA grafted PVDF membrane.

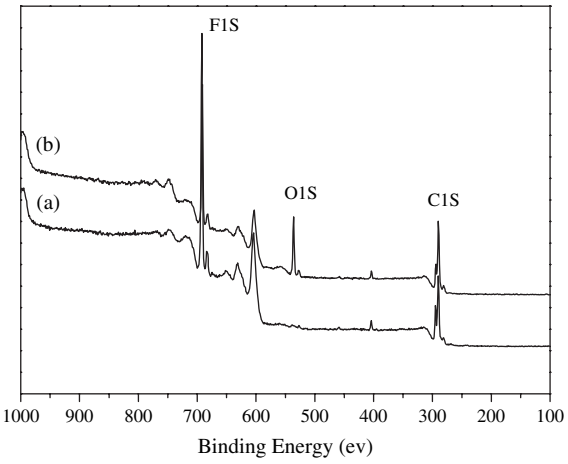

Fig. 5. XPS survey scan spectra of (a) original membrane and (b) 6.63 wt% PEGMA grafted PVDF membrane.

onto the membrane surface. The near-surface mole fraction of PEGMA 0.15 calculated as

$$\frac{[\mathrm{PEGMA}]}{[\mathrm{PEGMA}]+[\,-\mathrm{CH_2CF_2}-\,]}=\frac{A_{\mathrm{COO}}}{A_{\mathrm{COO}}+A_{\mathrm{CF_2}}},$$

where A_{COO} and $A_{\mathrm{CF_2}}$ are areas of the COO and CF_2 peak components, was higher than the bulk mole fraction of PEGMA 0.04 calculated as

$$\frac{G\%/1100}{G\%/1100+(1-G\%)/64},$$

where $G\%$ is the degree of grafting of PVDF membrane. As can be seen in Fig. 6(b) O1s could also be resolved into three peaks corresponding to C–O, C=O and O–C=O with binding energy at 536.2, 535.8 and 537.1 eV, respectively, which further confirm the successful immobilization of PEGMA comb-like polymer brushes on the PVDF membrane surface.

To further study the chemical structure changes of the grafted membrane, ^{1}H NMR and ^{13}C NMR were both performed on the solution of grafted PVDF membrane in deuterated dimethyl sulfoxide ($(CD_3)_2SO$). In Fig. 7(a), the characteristic multiplet centered at 2.9 ppm and 2.3 ppm is assigned to methylene groups, arising from the well-known tail-to-head (th) and tail-to-tail (tt) bonding arrangements, respectively. The chemical shifts at 2.5 ppm and 3.4 ppm are attributable to the solvent peak and residual H_2O peak. The peak appearances of the chemical shifts at 3.5 ppm and 3.2 ppm are assigned to the OCH_2 group and OCH_3 end group, indicating the presence of the grafted PEGMA side chains. The bulk mole fractions of PEGMA in the PVDF-*g*-PEGMA membrane were 0.01 calculated as

$$\frac{\frac{1}{9\mathrm{I}}(I_{\mathrm{OCH_2}}+I_{\mathrm{OCH_3}})}{\frac{1}{9\mathrm{I}}(I_{\mathrm{OCH_2}}+I_{\mathrm{OCH_3}})+\frac{1}{2}\left(I_{\mathrm{CH_2(th)}}+I_{\mathrm{CH_2(tt)}}\right)},$$

which is comparable to the value calculated by the gravimetric method. From ^{13}C spectra of PVDF-*g*-PEGMA in Fig. 7(b), we could see the chemical shifts at 120.7 ppm for CF_2 resonance and 43.5 ppm for CH_2. The chemical shifts at 165.8 ppm and 70.5 ppm are attributable to $-C{=}O$ and $-CH_2O$ groups, which can further verify the presence of the grafted PEGMA chains. Compared the surface mole fraction of PEGMA from XPS analysis with the bulk mole fraction from ^{1}H NMR, it could be concluded that the side chains (PEG) of grafted PEGMA would stretch out of the membrane surface due to the special comb-like architectures.

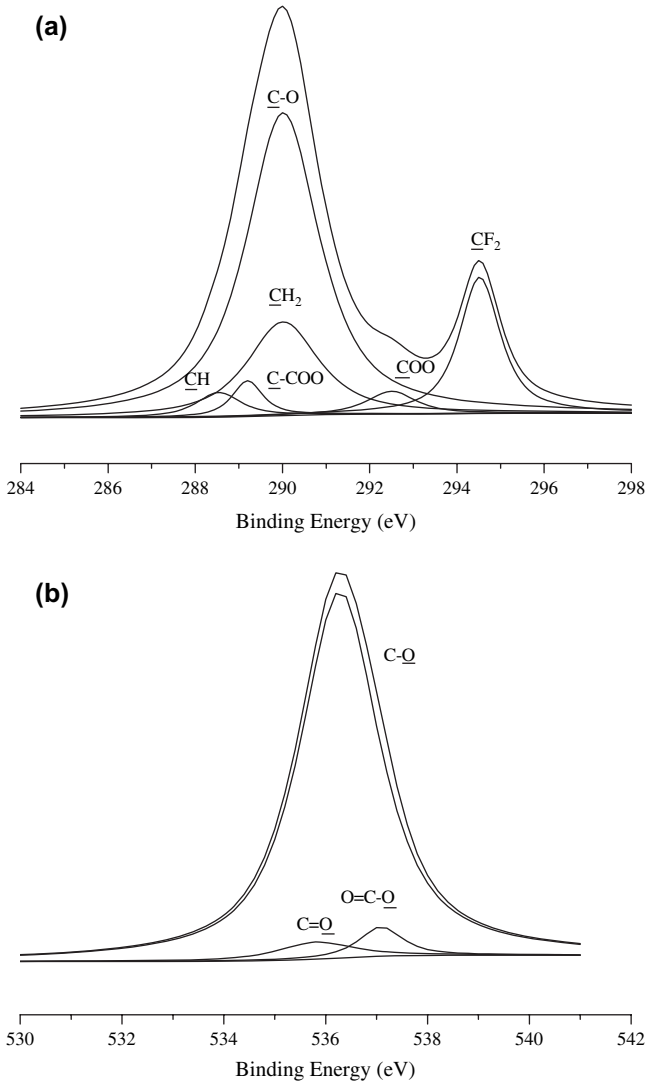

Fig. 6. XPS (a) the C1s core level scan spectra and (b) the O1s core level scan spectra of the PVDF-*g*-PEGMA membrane.

3.3. The membrane morphology and structure characterization

The membrane SEM morphological changes can be seen in Fig. 8. No significant morphological changes were observed on the membrane cross section (A3 and B3). The upper surface (A1 and B1) is nearly plugged by the grafted polymer brushes. The pores of the bottom surface (A2 and B2) are slightly narrowed. From the three-dimensional AFM pictures

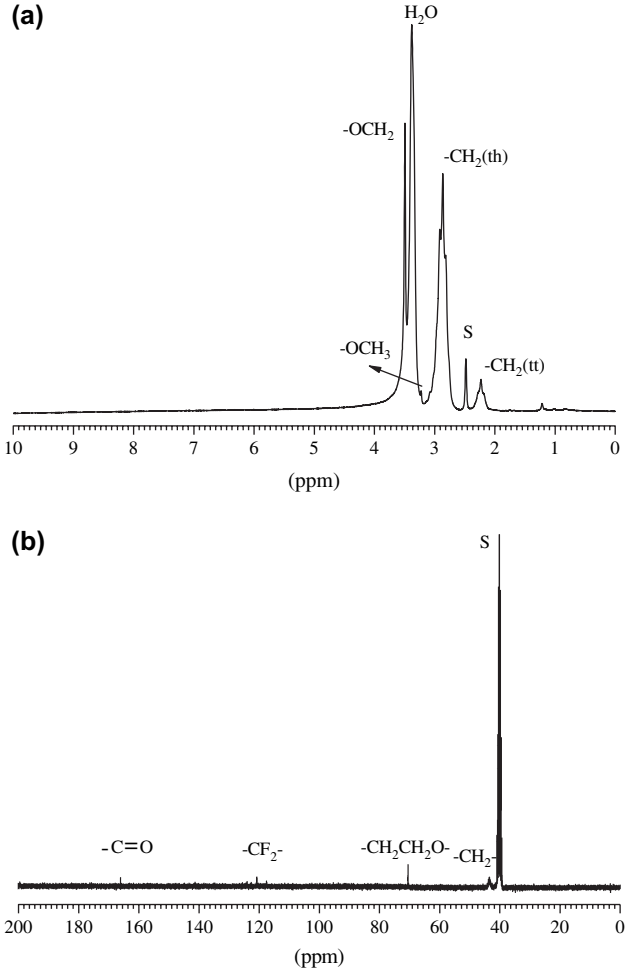

Fig. 7. (a) 300 MHz ^{1}H NMR and (b) 75 MHz ^{13}C NMR spectra for the 6.63 wt% PVDF-*g*-PEGMA membrane.

in Fig. 9, we can see that the surface root mean square (RMS) roughness of the grafted membrane increase from 5.638E + 01 nm to 1.843 + 02 nm based on 20 μm × 20 μm scan area due to the presence of the grafted PEGMA brushes. So from the morphology changes also supported by the XPS and NMR results, we could conclude that the hydrophilic PEGMA chains were mainly grafted onto the surface of the PVDF porous membrane. From Table 1, we could see that the average bulk pore diameter increases slightly from 0.2669 μm to 0.4746 μm, it might because that the electron beam irradiation induces the chain scissions especially in the crystalline–amorphous interphase regions in the PVDF causing an increase in molecular chains mobility [41]. The increasing movement of the PVDF chains in the amorphous region under the electron beam irradiation results in the chains' crosslinking to some extent. So the chains' movement under irradiation and the appropriate crosslinking increase the bulk pore size slightly. Besides, we have known that PEGMA chains were mainly grafted onto the PVDF membrane surface and did not influence the internal pores. So the internal pore blockage phenomenon that usually arises in most case of membrane surface grafting could be avoided at the lower degree of grafting. The porosity of the membrane decreases from 75.56% to 73.73%, which means that the membrane bulk structure keeps almost unchanged even after being grafted.

DSC thermograms in Fig. 10 show that the PVDF-*g*-PEGMA membrane has a little depressed melting temperature 159.4 °C compared with 161.2 °C for the PVDF membrane indicating the excellent thermal stability of PVDF membrane even after electron beam treatment. The calculated percent crystallinity is reduced from 35.9% in PVDF membrane to 33.1% in PVDF-*g*-PEGMA membrane, as indicated by the variation of the heat of melting. The depressed crystallinity of the grafted PVDF membrane might be expected due to the presence of amorphous PEGMA chains.

The mechanical properties of both original and grafted PVDF membranes might be the results of the structure and crystalline levels. PVDF crosslinks readily when exposed to radiation, Sands calculated the ratio of chain scission to crosslinking, $p_o/q_o = 0.47$ using the irradiated PVDF solubility data for the dose range of 100–1000 kGy [42]. The tensile strength of irradiated PVDF membrane will increase until a dose rise of 800 kGy, the percent elongation decreases gradually with the increase of irradiation dose [43,44]. The variation of the mechanical properties of the irradiated PVDF can be attributed to crystal disruption and crosslinking, which results in a limited movement of chain segments in the cross-linked structure of PVDF membranes. And similar results reported by Sands [42] can also prove that the irradiated PVDF membrane still have excellent mechanical properties for practical filtration application.

3.4. Hydrophilicity characterization

The relative hydrophilicity of the membrane can be obtained by water contact angle measurement. The initial static water contact angle was immediately measured when the water droplet was deposited on the membrane surface, which better reflects the natural wettability of the membrane material surface. As can be seen from Table 1, regardless of any side of the surface, the initial static water contact angles decrease significantly after being grafted for both upper and the bottom surfaces. However, only static contact angle measurements are difficult to interpret with the porous polymer membranes due to capillary forces, contraction in the dried state, structure rearrangements, heterogeneity and roughness of the surfaces. So the dynamic contact angle measurements were more reasonable to determine the polarity of the porous membrane surface. As shown in Table 1, both advancing and receding contact angles decreased obviously after being grafted. Moreover, the contact angle hysteresis, which is a measure of polymer chain dynamics occurring at the membrane surface, increased from 17.2–19.5° to 29.8–29.5°. It indicates that the hydrophilic grafted membrane has the less stable surface structure than the original membrane due to the presence of the grafted PEGMA chains. Furthermore, the contact angle hysteresis increase could also be attributed to the surface roughness increase, which could be seen from the above AFM results. Moreover, the bulk hydrophilicity of the membrane could be reflected by the dynamic adsorption process more reliably. As shown in Fig. 11, the contact angle of the

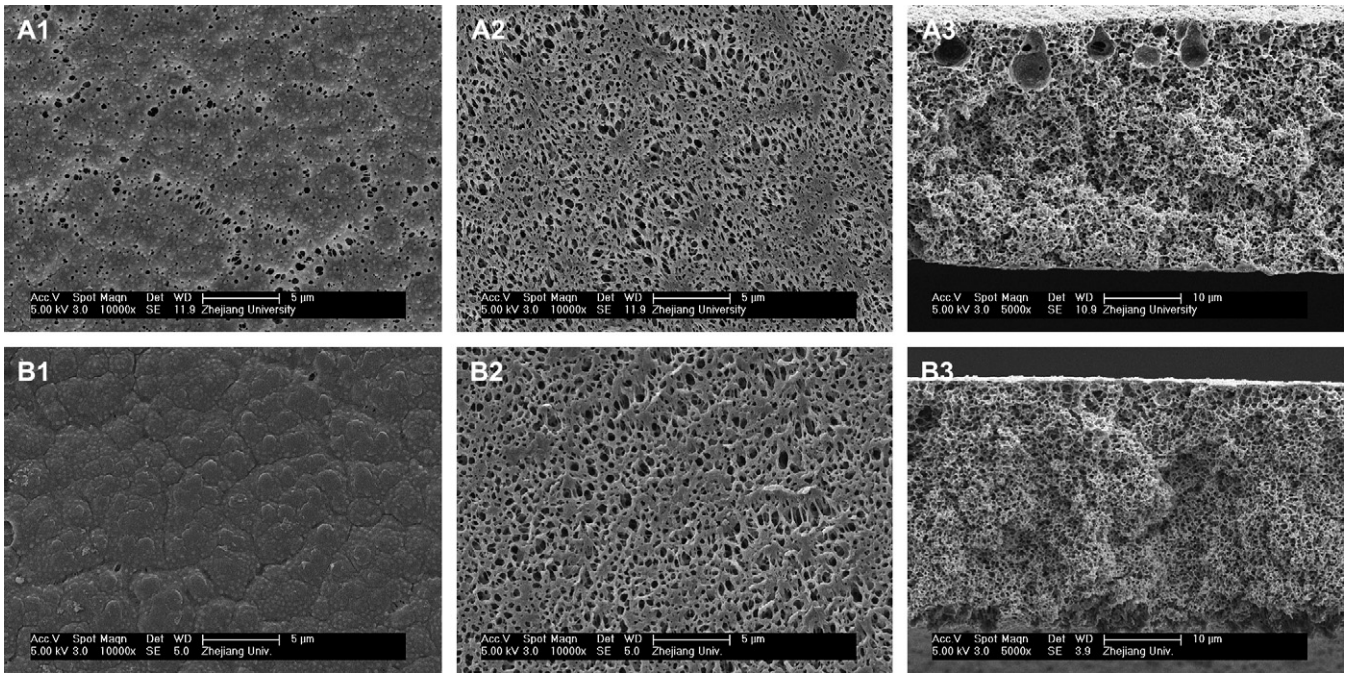

Fig. 8. SEM micrographs of original membrane (A1, A2, A3) and 6.63 wt% PEGMA grafted PVDF membrane (B1, B2, B3). A1, B1: upper surface; A2, B2: bottom surface; A3, B3: cross section.

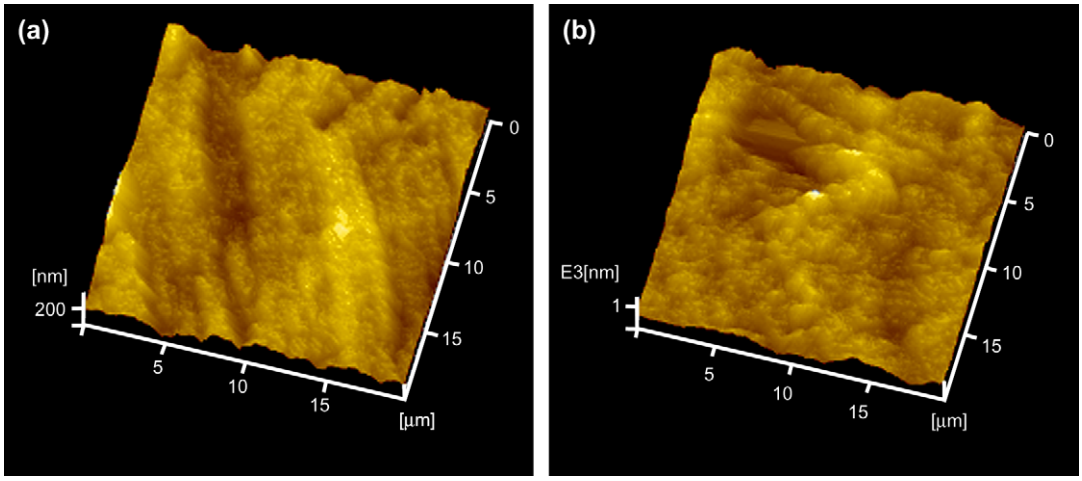

Fig. 9. Surface AFM images of (a) original membrane and (b) 6.63 wt% PEGMA grafted PVDF membrane.

original membrane almost keeps unchanged with the drop age, while the contact angles of the grafted membrane decrease significantly in the presence of PEGMA polymer brushes and more directly due to the hydrophilic nature of the PEG side chains. So the hydrophilicity of PVDF membrane could be improved significantly using the comb-like polymer brush architecture of grafted chains.

3.5. Filtration performance

To evaluate the flux changes and the fouling resistance of the grafted membrane, the pure water and BSA solution fluxes were measured, respectively [30,45]. In Table 1, the pure

Table 1
Structure and performance parameters of both original and grafted PVDF membranes

	Original membrane		Grafted membrane	
	Upper surface	Bottom surface	Upper surface	Bottom surface
Initial static angle θ_s	102.3	85.6	51.0	58.5
Advancing angle θ_a	91.2	86.2	60.6	62.8
Receding angle θ_r	74.0	66.7	30.8	34.3
Hysteresis angle $\theta_a - \theta_r$	17.2	19.5	29.8	28.5
Mean pore size (µm)	0.2669		0.4746	
Porosity (%)	75.56		73.73	
Flux (L/m^2 h)	180.4		226.1	

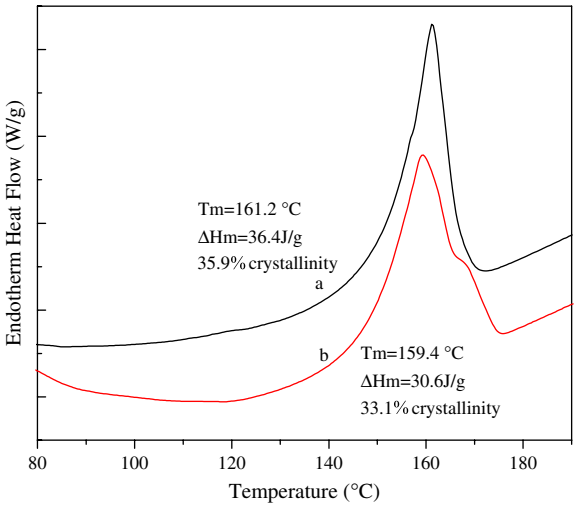

Fig. 10. DSC thermograms for PVDF membrane and PVDF-*g*-PEGMA membrane.

water flux of grafted membrane increased from 180.4 to 226.1 L/m^2 h. It mainly results from the improvement of the PVDF membrane hydrophilicity. The stretching and/or shrinking conformation of the grafted hydrophilic PEGMA chains immobilized onto the amorphous domain determines the permeability of water across the membrane through the pores. In addition, the increase of the mean pore size may also contribute to the flux change. Fig. 12 shows the relative ratio (J/J_0) of BSA solution flux normalized by the initial pure water flux based on the flux reductions due to the protein fouling alone. The variation of the flux ratio (J/J_0) with filtration time shows the degree of fouling of both original and grafted membrane. The flux of the original membrane declined rapidly to about 30% of the initial pure water flux in 3 h, while the flux of the grafted membrane still kept more than 85% of the initial case in 3 h. The surface grafted PVDF membrane thus exhibits a better antifouling property in the dynamic fouling process than that of the original hydrophobic PVDF membrane. This is because that

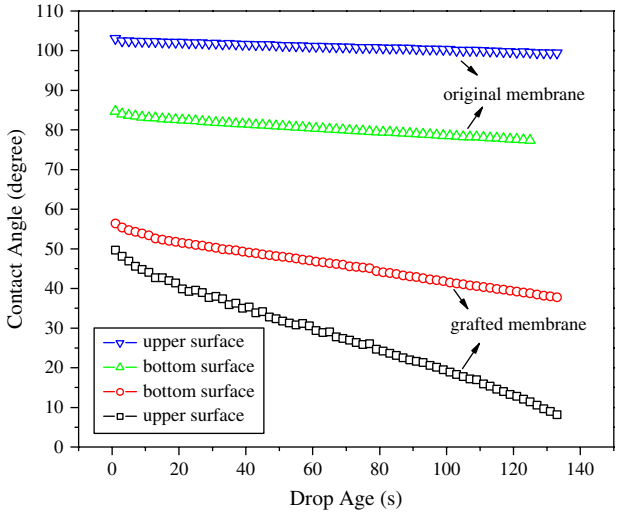

Fig. 11. Changes of contact angles with drop age for both original and grafted PVDF membranes.

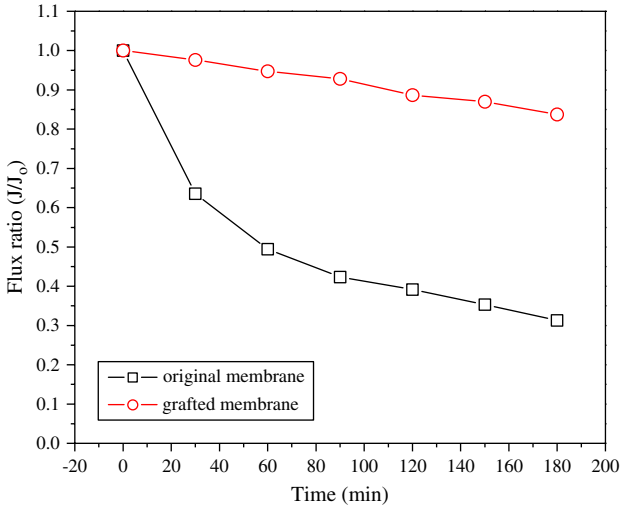

Fig. 12. Flux ratio of 1.0 g/L BSA solution (J) divided by initial pure water flux (J_0) as a function of filtration time for the original and grafted PVDF membranes.

the grafted hydrophilic PEGMA chains weaken the hydrophobic interactions between BSA molecules and PVDF membrane and affect the surface adsorption of BSA. To be specific, the hydrophilic PEG side chains have better biocompatibility, large excluded volume and unique coordination with surrounding water molecules in BSA aqueous solution. So the changes of BSA solution flux indicated the improvement in fouling resistance of the PVDF-*g*-PEGMA membrane.

4. Conclusion

PEGMA was grafted onto the surface of PVDF porous membrane by the pre-irradiation of electron beam to form a layer of comb-like polymer brushes. FTIR-ATR, XPS and NMR analysis demonstrated that PEGMA chains were mainly grafted onto the PVDF membrane surface and PEG side chains would spread on the membrane surface due to the special architecture, and the results were also supported by the SEM and AFM morphologies. Both the static contact angle and dynamic contact angle changes showed that the PEGMA grafted PVDF membrane possessed a better hydrophilicity, which could be further confirmed by the dynamic adsorption process of a water droplet on the membrane surface. The pure water and BSA solution flux changes indicated the filtration performance improvement of the grafted PVDF membrane with hydrophilic polymer brushes. These results proved that the hydrophilicity and fouling resistance of the PVDF membrane could be effectively improved by surface grafting of special comb-like PEGMA through electron beam irradiation.

Acknowledgement

Financial support from the National 973 Foundation of China (No. 2003.CB615705) and National Nature Science Foundation of China (No. 50433010) is gratefully appreciated and acknowledged.

References

[1] Dargaville TR, George GA, Hill DJT, Whittaker AK. Prog Polym Sci 2003;28:1355.
[2] Ortiz de Zárate JM, Peña L, Mengual JI. Desalination 1995;100:139.
[3] Bottino A, Capannelli G, Comite A. Desalination 2005;183:375.
[4] Srisurichan S, Jiraratananon R, Fane AG. J Membr Sci 2006;277:186.
[5] Khayet M, Matsuura T. Ind Eng Chem Res 2001;40:5710.
[6] Sun HX, Zhang L, Chai H, Yu J, Qian H, Chen HL. Separation Purification Technol 2006;48:215.
[7] Tsai YH, Wang MY, Suen SY. J Pharm B 2001;766:133.
[8] Souzy R, Ameduri B. Prog Polym Sci 2005;30:644.
[9] Holmberg S, Holmlund P, Nicolas R, Wilen CE, Kallio T, Sundholm G, et al. Macromolecules 2004;37:9909.
[10] Soresi B, Quartarone E, Mustarelli P, Magistris A, Ghiodelli G. Solid State Ionics 2004;166:383.
[11] Gupta Y, Hellgardt K, Wakeman RJ. J Membr Sci 2006;282:60.
[12] Chen H, Kovvali AS, Majumdar S, Sirkar KK. Ind Eng Chem Res 1999;38:3489.
[13] Liu YJ, Feng X, Lawless D. J Membr Sci 2006;271:114.
[14] Jian K, Pintauro PN. J Membr Sci 1993;85:301.
[15] Jian K, Pintauro PN. J Membr Sci 1997;135:41.
[16] Chang CL, Chang MS. J Membr Sci 2004;238:117.
[17] Howe KJ, Clark MM. Environ Sci Technol 2002;36:3571.
[18] Ghosh R. J Membr Sci 2002;195:115.
[19] Ho CC, Zydney AL. Ind Eng Chem Res 2001;40:1412.
[20] Kelly ST, Zydney AL. J Membr Sci 1995;107:115.
[21] Mueller J, Davis RH. J Membr Sci 1996;116:47.
[22] Güell C, Davis RH. J Membr Sci 1996;119:269.
[23] Ulbricht M. Polymer 2006;47:2217.
[24] Ochoa NA, Masuelli M, Marchese J. J Membr Sci 2003;226:203.
[25] Nunes SP, Peinemann KV. J Membr Sci 1992;73:25.
[26] Lin DJ, Chang CL, Lee CK, Cheng LP. Eur Polym J 2006;42:2407.
[27] Yang MC, Liu TY. J Membr Sci 2003;226:119.
[28] Lu Y, Yu SL, Chai BX, Shun XD. J Membr Sci 2006;276:162.
[29] Hester JF, Banerjee P, Won YY, Akthakul A, Acar MH, Mayes AM. Macromolecules 2002;35:7652.
[30] Chen YW, Ying L, Yu WH, Kang ET, Neoh KG. Macromolecules 2003;36:9451.
[31] Forsythe JS, Hill DJT. Prog Polym Sci 2000;25:101.
[32] Seguchi T, Makuuchi K, Suwa T, Tamura N, Abe T, Takehisa MJ. Chem Soc Jpn Chem Ind Chem 1974;7:1309.
[33] Clochard MCL, Begue J, Lafon A, Caldemaison D, Bittencourt C, Pireaux JJ, et al. Polymer 2004;45:8683.
[34] Liu F, Zhu BK, Xu YY. Appl Surf Sci 2006;253:2096.
[35] Mazzei R, Smolko E, Tadey D, Gizzi L. Nucl Instr Meth Phys Res B 2000;170:419.
[36] Flint SD, Slade RCT. Solid State Ionics 1997;97:299.
[37] Brandrup J, Immergut EH, Grulke EA. Polymer handbook. New York: John Wiley & Sons; 1999.
[38] Chen H, Belfort G. J Appl Polym Sci 1999;72:1699.
[39] Mohamed MN, Hamdani S. J Membr Sci 2003;216:27.
[40] Robinson DN, Peppas NA. Macromolecules 2002;35:3668.
[41] Zhudi Z, Jin C, Xinfang C. Radiat Phys Chem 1994;43:523.
[42] Sands GD, Pezdirz GF. Polym Prepr 1965;6:987.
[43] Nasef MM, Hamdani S, Dahlan KZM. Polym Degrad Stab 2002;75:85.
[44] Nasef MM, Dahlan KZM. Nucl Instr Meth Phys Res B 2003;201:604.
[45] Dai ZW, Nie FQ, Xu ZK. J Membr Sci 2005;264:20.